Applied Physics Letters

Generation of nanosecond THz pulses using a high gain ring resonator with a semiconductor switch

Cite as: Appl. Phys. Lett. **121**, 044101 (2022); https://doi.org/10.1063/5.0098718
Submitted: 11 May 2022 • Accepted: 09 July 2022 • Published Online: 27 July 2022

J. Genoud, E. L. Claveau, S. K. Jawla, et al.

Applied Physics Letters ARTICLE scitation.org/journal/apl

Generation of nanosecond THz pulses using a high gain ring resonator with a semiconductor switch

Cite as: Appl. Phys. Lett. **121**, 044101 (2022); doi: 10.1063/5.0098718
Submitted: 11 May 2022 · Accepted: 9 July 2022 ·
Published Online: 27 July 2022

J. Genoud,[a] E. L. Claveau, S. K. Jawla, G. Li, J. F. Picard, M. A. Shapiro, and R. J. Temkin

AFFILIATIONS

Plasma Science and Fusion Center, Massachusetts Institute of Technology, Cambridge, Massachusetts 02139, USA

[a]Author to whom correspondence should be addressed: genoud@mit.edu

ABSTRACT

A 250 GHz quasi-optical ring resonator consisting of an input coupler and three mirrors has been designed and tested. A low-loss silicon wafer in the ring provides output coupling of the stored power when irradiated by a pulse from a 532 nm laser. The ring created 5.8 ns, 268 mW output power pulses when excited by a 17 mW, 250 GHz continuously operating input source, achieving a power gain of 16. In a fully tuned ring, higher gain is achievable. If the ring was used with a pulsed input source having a pulse length of several times the fill time, the ring could be used as an efficient pulse compressor with similar high gain. The resonator has a wide range of applications, including, at low power, spectroscopy and, at high power, testing of accelerator structures and materials.

High power pulses on the nanosecond timescale are needed in the millimeter wave (MMW) and THz range for both low- and high-power applications. At low power, they are used to increase the signal to noise ratio in spectroscopy, for example, in dynamic nuclear polarization nuclear magnetic resonance (DNP-NMR) spectroscopy.[1,2] At high power, nanosecond pulses are used for powering and studying breakdown in MMW/THz accelerators[3] or at the surface of materials. The direct generation of high power pulses on a nanosecond timescale is challenging because of the need to achieve nanosecond rise and fall times. Because pulses on the microsecond scale are much easier to generate and are more efficient, it is very attractive to compress such pulses to increase the available power and generate pulses on the nanosecond scale. The present research demonstrates a 250 GHz, high gain pulse compressor based on a resonant ring and a laser-driven semiconductor switch (LDSS).

Resonant rings, pulse compressors, and laser-driven semiconductor switches have been extensively studied over a wide range of frequencies. Resonant rings are used to generate high field strengths in order to test microwave components within the ring.[4] The study of such rings has been extended to the millimeter wave region, for example, near 34,[5] 50,[6] 140 GHz,[7] and in the THz region.[8,9] In the majority of these cases, the power inside the ring was greatly increased in comparison to the input source, which permits internal testing of components, but the power was not coupled out to demonstrate a high gain, compressed output. A two-mirror resonator with an internal silicon wafer driven by a laser switch had been previously demonstrated to generate subnanosecond high-power far-infrared pulses.[9]

Major advances in pulse compressors have been made in the microwave region, especially at the X-band, including the SLED system and its recent improvement using overmoded waveguides[10] or storage cavities.[11,12] The SLAC Energy Doubler (SLED)-type compressors intentionally operate at modest gain, about 4–8, and use a phase reversal of the input power to generate the output pulse. Pulse compressors for accelerator applications have also been demonstrated at a frequency as high as 34 GHz using phase reversal, phase shifting, or plasma discharge tubes.[13–15] Along with advances in experiment, the theory of ring-based pulse compressors has also been studied.[4,16–19]

Separately, laser-driven semiconductor switches have been studied experimentally at frequencies up through the THz range, including early research such as Refs. 20–22 and recent research at 110,[23] 240,[24] and 260 GHz.[25] Theoretical research has also been conducted on these switches.[26,27]

The present results differ from the prior research in demonstrating a complete, high gain resonant ring generating nanosecond-scale output pulses at a higher frequency, 250 GHz, than in prior research.

The ring resonator setup scheme is shown in Fig. 1. The schematic is not drawn to scale; the electric field at the mirror edge is reduced by 27 dB. The 250 GHz source provides up to 20 mW. The ring consists of three gold-coated elliptical mirrors and one planar input coupler. The focal lengths of the three mirrors are, respectively,

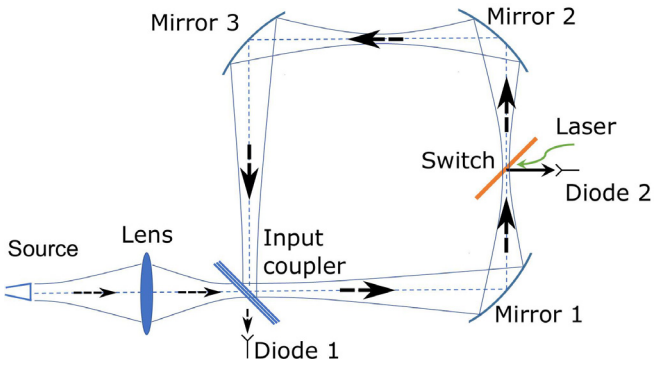

FIG. 1. Schematic of the ring resonator (not drawn to scale).

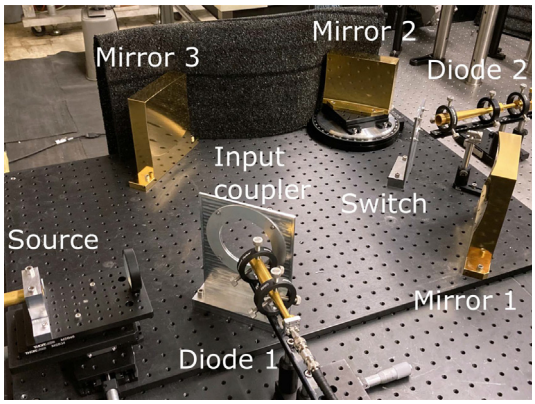

FIG. 2. Photograph of the ring resonator.

157, 218, and 473 mm The distance between each of these elements is 430 mm. The input coupler is a set of three parallel fused silica disks set at 45° with respect to the incoming wave. The distance between the disks is adjustable, allowing it to tune the input coupler transmissivity/reflectivity. The coupler is designed to transmit only a small fraction of the input power, typically below 10%. The millimeter wave beam is polarized in the vertical direction, perpendicular to the plane of the ring.

The operation of the ring resonator requires the phase to match between the wave transmitted into the ring through the input coupler and the wave kept inside the ring by reflection on the input coupler. This phase matching condition is achieved by slightly adjusting the position of the mirrors with micrometer translation stages and/or by adjusting the wave frequency.

The power is extracted with the output coupler located between mirrors 1 and 2. The output coupler is a silicon wafer of 0.361 mm thickness set at 45° with respect to the wave. In normal conditions, the wafer is transparent to the 250 GHz rf-wave. The rf-wave is reflected outside the ring when the wafer is irradiated with a laser pulse. The laser used is a Quantel Q-smart 450 Q-switched Nd:YAG laser with a frequency doubling stage, producing a 6 ns, 230 mJ pulse at 532 nm. The properties of a Si wafer switch driven by this laser and operated at 110 GHz have been previously reported.[23] The source is continuously feeding the ring resonator, up to the point where the overall losses balance the input power. When the switch is irradiated by the laser, the rf-wave exits the ring in a time corresponding to the round trip time in the ring. Instead of being used in with a cw input source, the ring can be used with a pulsed input source with pulses of several times the fill time. In this case, the ring resonator will act as a pulse compressor with high gain.

A photo of the ring resonator is shown in Fig. 2. The laser is located on the right, outside the photo field of view. Two Schottky diodes are used as diagnostics. They are located outside the ring resonator. The first one (diode 1 in Fig. 2) measures the power reflected by the input coupler. This diode is used mainly during the alignment and tuning processes. It provides a measurement of the reflected power while the ring power is increasing. The second diode (diode 2) monitors the power reflected by the semiconductor switch. This diode provides the power measurement when the silicon wafer is irradiated and the wave is reflected outside the ring.

In this paper, all of the results presented are obtained with an input coupler composed of three 0.18 mm thick fused quartz disks, spaced by 0.4 mm. In this configuration, the reflection of the input coupler is 97%, allowing 3% of the power into the ring. However, care must be taken to couple the transmitted power to the mode inside the ring. The efficiency of coupling is determined by analyzing the ring performance.

As an illustration, the signals measured during a typical pulse are reported in Fig. 3.

The dashed line in the figure indicates the time when the 250 GHz source is triggered. After this, the signal from diode 1

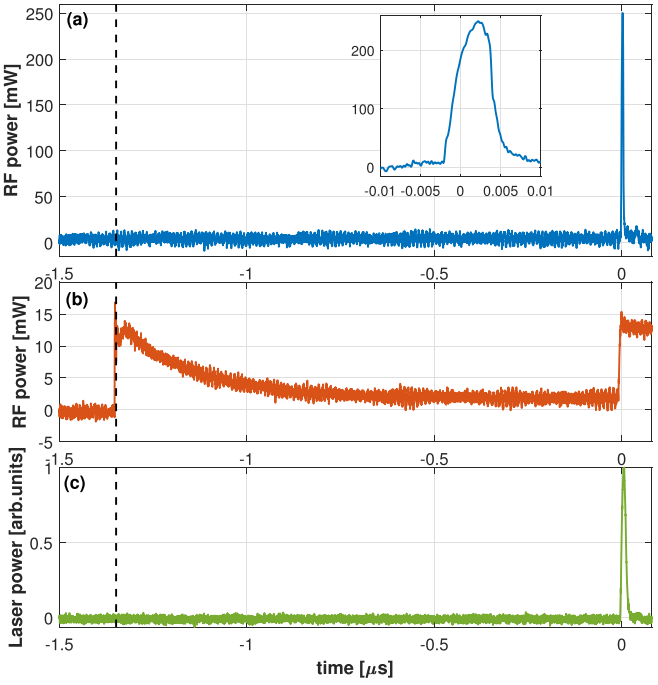

FIG. 3. (a) RF power measured at diode 2 exiting the ring by reflecting on the semiconductor wafer vs time. (b) RF power measured by diode 1. (c) Laser power measured outside the ring.

increases immediately. This is the signal of the wave directly reflected by the input coupler. In this configuration, 97% of the power is directly reflected toward diode 1 and 3% of the power is entering the ring. After this initial transition, the ring is filling up gradually. This can be seen by the decrease in the signal measured on diode 1, which eventually reaches a very low level when the cavity is filled. This is an indication of the good phase and amplitude matching between the wave coming from the source and the wave reflected by the input coupler inside the ring. For the example shown in Fig. 3, the laser was fired about 1.3 μs after the start of the filling of the ring. This time is labeled $t = 0$ s. At that time, the wafer reflects the power out. Diode 2 measures the high-power signal, as seen in Fig. 3(a). The rf-wave exits the ring in a time corresponding to the round trip time in the ring. For this ring, the length is 1.7 m, leading to an output power pulse length of 5.8 ns. This can be seen in the inset in Fig. 3(a). For this pulse, the full width at half maximum of the power is 4.8 ns.

The ring can be optimized by reducing the different losses such as misalignment losses or by varying the transmissivity of the input coupler. The alignment of all the elements is performed with the help of an optical laser. After the alignment, the ring cavity is tuned by sweeping the source rf-frequency. This allows finding the best performance settings. In this case, the best performance is found at 251.215 GHz. The signal measured at the output of the ring resonator during the frequency sweeping process with 17 mW of input power is shown in Fig. 4. The outcome is in the form of a resonance shape with a maximum measured output power from the ring of 268 mW. The maximum gain is $286/17 = 16$.

In Fig. 5, the measured rf output power for different laser trigger times is shown. The laser trigger time is counted starting at the same time as the source trigger time. An example of the output power signal for $t_{laser} = 1.3$ μs is presented in Fig. 3. At $t_{laser} = 0$ s, the laser is triggered at the same time as the source. It is shown that the power stored in the ring is nearly saturated after 1 μs and is fully saturated after 1.5 μs. For this case, the ring resonator was not as finely optimized as in the previous case shown in Fig. 4. The maximum output power in Fig. 5 is 246 mW, and the maximum power gain is $246/17 = 14.5$.

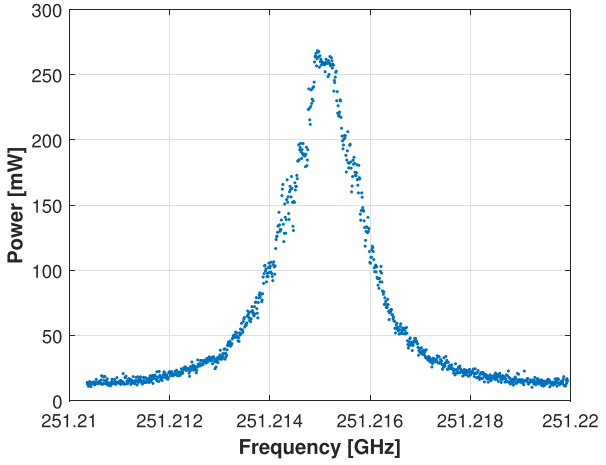

FIG. 4. Resonance peak of the ring resonator around 251.215 GHz.

The difference from the data of Fig. 4 is likely due to a small misalignment of the different elements in the ring resonator that arose between taking the two sets of data.

The power stored in a ring resonator as a function of time is given by[17]

$$\frac{P_{ring}}{P_0} = \frac{\omega_0 c}{Q_c L}\left(\frac{2Q_{tot}}{\omega_0}\right)^2\left(1 - \exp\left(-\frac{\omega_0 t}{2Q_{tot}}\right)\right)^2, \quad (1)$$

where P_0 is the incident power, P_{ring} is the power inside the ring, ω_0 is the frequency, Q_c is the coupling quality factor, Q_{tot} is the total quality factor of the ring, c is the speed of light, $L = 1.7$ m is the ring total length, and t is the time after the beginning of the filling of the ring. The total Q of the ring is given by $Q_{tot}^{-1} = Q_c^{-1} + Q_{loss}^{-1}$, where $Q_c = \frac{kL}{T_{in}^2}$, $Q_{loss} = \frac{kL}{\alpha}$, $k = \frac{\omega_0}{c}$, T_{in}^2 is the power transmissivity of the coupler, and α is the dimensionless loss per round trip of the power circulating inside the cavity.

We can determine the ring parameters using the curve in Fig. 5. The curve is a measurement of the power in the ring, P_{ring}, after reflection from the Si wafer. The measured output power is then $P_{out} = RP_{ring}$, where R is the power reflectivity of the Si wafer when irradiated. A reflectivity R of 0.81 was separately measured; this is a higher value than achieved in our prior research that used a silicon wafer with a rapid recombination time.[23] Using Eq. (1) and the time dependence of the curve in Fig. 5, we obtain an estimated total quality factor of $Q_{tot} = 2.05 \times 10^5$.

Using $P_{ring} = P_{out}/R$ and the value of Q_{tot} in Eq. (1), we obtain a coupling quality factor of $Q_c = 1.05 \times 10^6$ and a loss Q of $Q_{loss} = 2.54 \times 10^5$. The power loss per round trip is $\alpha = 0.035$, and the power transmission of the input wave is $T_{in}^2 = 8.5 \times 10^{-3}$. The uncertainty on these parameters is estimated to be on the order of 10%. The limiting factors of this prototype are the alignment errors, the stability of the whole setup, and the sensitivity to temperature change.

The repetition rate of the ring resonator operation is a key factor in applications such as DNP-NMR spectroscopy or for accelerator structure testing. As such, it is important to define the laser energy

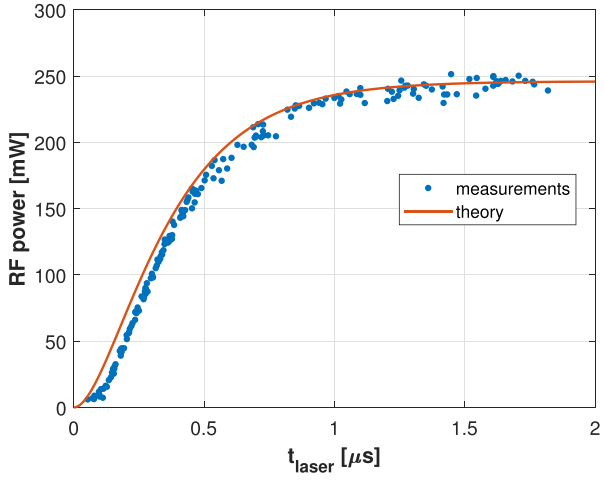

FIG. 5. Measured output power vs laser trigger time (blue dots) and the best fit to the data using Eq. (1) (red line). At $t_{laser} = 0$, the laser is triggered at the same time as the rf source.

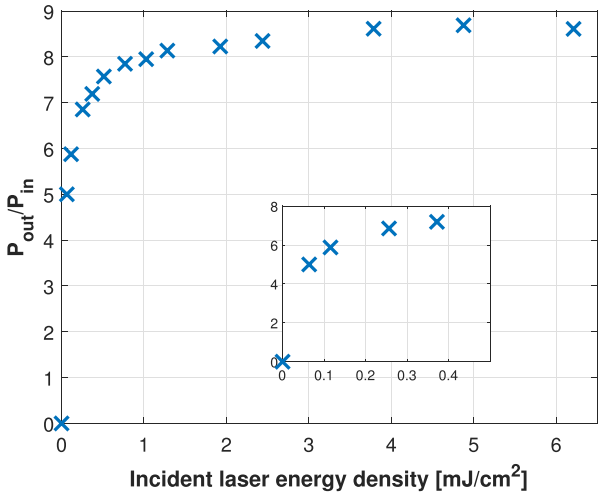

FIG. 6. Ratio between output and input power vs the incident laser energy density on the semiconductor wafer.

requirement for wafer irradiation. The ratio between the output power of the ring P_{out} and the source power P_{in} as a function of the incident laser energy density on the semiconductor wafer is shown in Fig. 6. Note that this measurement has been done at a different operating point than the best performance operating point presented before. The maximum gain in this case is 8.7. The wafer surface area irradiated by the laser is 7.8 cm^2. This measurement indicates that using only 2.3 mJ (or 0.3 mJ/cm^2) of the incident laser energy density on the wafer permits to get a gain of 7, or equivalently 80% of the maximum rf-wave power circulating in the ring.

In conclusion, the design and testing of a 250 GHz quasi-optical ring resonator are reported. The initial tests are promising and demonstrate an overall power gain of up to 16. By optimizing the cavity, the gain could be further increased. The power stored in the ring is optimized when critical coupling is achieved, that is, when the coupling Q (Q_c) is equal to the loss Q (Q_{loss}). The input coupler used in the ring has variable coupling so that, in principle, it could be adjusted to achieve critical coupling. The input coupler was adjusted to achieve 3% transmission, but the transmitted power coupled to the field inside the ring was measured to have an effective value of $T_{in}^2 = 8.5 \times 10^{-3}$. This would indicate that the input power did not fully couple to the mode inside the ring. This may be caused by misalignments or by the use of an input coupler consisting of three plates with multiple internal reflections. The internal loss per round trip in the ring was measured to be $\alpha = 0.035$. Our calculated loss per round trip inside the ring is 0.002 from Ohmic loss, 0.0134 from cross-polarization loss, and 0.0050 from distortion loss[28] for a total expected value of $\alpha = 0.0205$. The losses due to dielectric absorption, beam walk-off in the quartz plates forming the input coupler, and misalignment[29] have not been estimated and could explain the disagreement between the calculated and measured values.

The maximum power gain of a ring occurs for critical coupling ($Q_c = Q_{loss}$) and is given by α^{-1} which for our ring equals 29. If a Si wafer reflectivity of R = 1 were achieved and the input coupling optimized, a ring gain of 29 could be obtained.

The alignment accuracy, the stability of the whole setup, and the sensitivity to temperature change have been identified as the likely factors limiting the power gain inside the ring. The wave is coupled out of the ring via a semiconductor switch, becoming reflective when irradiated with a laser. It is reported that an incident laser energy density of 0.3 mJ/cm^2 on the semiconductor wafer is sufficient to reach 80% of the maximum ring gain performance. Future effort will be directed to achieve these higher gain values. An application of this setup could be in combination with a 250 GHz gyro-amplifier for DNP-NMR spectroscopy applications.[30] A higher power version of the ring resonator could be utilized to test accelerating structures.[3]

This work was supported by the National of Institutes of Health (NIH) National Institute of Biomedical Imaging and Bioengineering (NIBIB) via Grant Nos. R01-EB001965 and R01-EB004866, by DOE HEP via Grant No. DESC0015566, and by DOE FES via Grant No. DE-FC02-93ER54186.

AUTHOR DECLARATIONS

Conflict of Interest

The authors have no conflicts to disclose.

Author Contributions

Jérémy Genoud: Conceptualization (lead); Formal analysis (lead); Investigation (lead); Methodology (lead); Writing – original draft (lead); Writing – review and editing (lead). **Elliot L. Claveau:** Conceptualization (equal); Formal analysis (equal); Investigation (equal); Methodology (equal). **Sudheer Jawla:** Conceptualization (equal); Formal analysis (equal); Investigation (equal); Methodology (equal). **Guangjiang Li:** Conceptualization (equal); Formal analysis (equal); Investigation (equal); Methodology (equal). **Julian Tesch Picard:** Conceptualization (equal); Formal analysis (equal); Investigation (equal); Methodology (equal). **Michael A. Shapiro:** Conceptualization (equal); Formal analysis (equal); Investigation (equal); Methodology (equal); Supervision (equal); Writing - original draft (equal); Writing - review & editing (equal). **Richard J. Temkin:** Conceptualization (equal); Formal analysis (equal); Investigation (equal); Methodology (equal); Supervision (lead); Writing - original draft (equal); Writing – review and editing (equal).

DATA AVAILABILITY

The data that support the findings of this study are available from the corresponding author upon reasonable request.

REFERENCES

[1]A. Abragam and M. Goldman, Rep. Prog. Phys. **41**, 395–467 (1978).
[2]L. R. Becerra, G. J. Gerfen, R. J. Temkin, D. J. Singel, and R. G. Griffin, Phys. Rev. Lett. **71**, 3561–3564 (1993).
[3]M. A. K. Othman, J. Picard, S. Schaub, V. A. Dolgashev, S. M. Lewis, J. Neilson, A. Haase, S. Jawla, B. Spataro, R. J. Temkin, S. Tantawi, and E. A. Nanni, Appl. Phys. Lett. **117**(7), 073502 (2020).
[4]S. J. Miller, Microwave J. **3**(9), 50–58 (1960).
[5]A. Bogdashov, G. Denisov, D. Lukovnikov, Y. Rodin, and J. Hirshfield, IEEE Trans. Microwave Theory Tech. **53**, 3152–3155 (2005).
[6]T. S. Bigelow, in *International Conference on Millimeter and Submillimeter Waves and Applications* (SPIE, 1994), pp. 320–321.
[7]G. G. Denisov and M. Y. Shmelyov, Int. J. Infrared Millimeter Waves **12**, 1187–1194 (1991).

[8]P. F. Goldsmith, *Quasioptical Systems: Gaussian Beam Quasioptical Propagation and Applications* (IEEE Press, New York, 1998).
[9]J. Burghoorn, J. P. Kaminski, R. C. Strijbos, T. O. Klaassen, and W. T. Wenckebach, J. Opt. Soc. Am. B **9**, 1888–1891 (1992).
[10]S. G. Tantawi, Phys. Rev. Spec. Top.-Accel. Beams **7**, 032001 (2004).
[11]J. W. Wang, S. G. Tantawi, C. Xu, M. Franzi, P. Krejcik, G. Bowden, S. Condamoor, Y. Ding, V. Dolgashev, J. Eichner, A. Haase, J. R. Lewandowski, and L. Xiao, Phys. Rev. Accel. Beams **20**, 110401 (2017).
[12]Y. Jiang, H. Zha, P. Wang, J. Shi, H. Chen, W. L. Millar, and I. Syratchev, Phys. Rev. Accel. Beams **22**, 082001 (2019).
[13]Y. Y. Danilov, S. V. Kuzikov, V. G. Pavel'ev, Y. I. Koshurinov, and S. M. Leshinsky, Tech. Phys. Lett. **27**, 803–805 (2001).
[14]O. A. Ivanov, A. A. Vikharev, A. M. Gorbachev, V. A. Isaev, M. A. Lobaev, A. L. Vikharev, S. V. Kuzikov, J. L. Hirshfield, and M. A. LaPointe, Phys. Rev. Spec. Top.-Accel. Beams **12**, 093501 (2009).
[15]A. A. Vikharev, G. G. Denisov, V. V. Kocharovsky, S. V. Kuzikov, V. V. Parshin, N. Y. Peskov, A. N. Stepanov, D. I. Sobolev, and M. Y. Shmelev, Radiophys. Quantum Electron. **50**, 786–793 (2007).
[16]L. J. Milosevic and R. Vautey, IRE Trans. Microwave Theory Tech. **6**, 136–143 (1958).
[17]R. A. Alvarez, Rev. Sci. Instrum. **57**, 2481–2488 (1986).
[18]J. L. Altman, *Microwave Circuits* (D. Van Nostrand Company, New York, 1964).
[19]B. J. Fox, B. Y. Rock, and R. J. Vernon, in *38th International Conference on Infrared, Millimeter, and Terahertz Waves (IRMMW-THz)* (IEEE, 2013).
[20]T. Nozokido, H. Minamide, and K. Mizuno, Electron. Commun. Jpn. **80**, 1–9 (1997).
[21]A. Johnson and D. Auston, IEEE J. Quantum Electron. **11**, 283–287 (1975).
[22]J. P. Kaminski, J. S. Spector, C. L. Felix, D. P. Enyeart, D. T. White, and G. Ramian, Appl. Phys. Lett. **57**, 2770–2772 (1990).
[23]J. F. Picard, S. C. Schaub, G. Rosenzweig, J. C. Stephens, M. A. Shapiro, and R. J. Temkin, Appl. Phys. Lett. **114**(16), 164102 (2019).
[24]S. Takahashi, L. Brunel, D. T. Edwards, J. van Tol, G. Ramian, S. Han, and M. S. Sherwin, Nature **489**, 409–413 (2012).
[25]M. L. Kulygin, G. G. Denisov, E. A. Novikov, A. P. Fokin, and I. A. Litovsky, Radiophys. Quantum Electron. **61**, 603–613 (2019).
[26]T. Vogel, G. Dodel, E. Holzhauer, H. Salzmann, and A. Theurer, Appl. Opt. **31**, 329–337 (1992).
[27]S. C. Schaub, Z. W. Cohick, and B. W. Hoff, Rev. Sci. Instrum. **92**, 113106 (2021).
[28]J. A. Murphy, Int. J. Infrared Millimeter Waves **8**, 1165–1187 (1987).
[29]P. F. Goldsmith, IEEE Trans. Microwave Theory Tech. **30**, 820–823 (1982).
[30]E. A. Nanni, S. Jawla, S. M. Lewis, M. A. Shapiro, and R. J. Temkin, Appl. Phys. Lett. **111**(23), 233504 (2017).